

Decreased Hepatic Futile Cycling Compensates for Increased Glucose Disposal in the *Pten* Heterodeficient Mouse

Jun Xu,¹ Lori Gowen,² Christian Raphaelides,² Katrina K. Hoyer,³ Jason G. Weinger,³ Mathilde Renard,³ Joshua J. Troke,³ Bhavapriya Vaitheeswaran,¹ W.N. Paul Lee,⁴ Mohammed F. Saad,⁵ Mark W. Sleeman,² Michael A. Teitell,^{3,6} and Irwin J. Kurland^{1,7}

Despite altered regulation of insulin signaling, *Pten*^{+/-} heterodeficient standard diet-fed mice, ~4 months old, exhibit normal fasting glucose and insulin levels. We report here a stable isotope flux phenotyping study of this “silent” phenotype, in which tissue-specific insulin effects in whole-body *Pten*^{+/-}-deficient mice were dissected in vivo. Flux phenotyping showed gain of function in *Pten*^{+/-} mice, seen as increased peripheral glucose disposal, and compensation by a metabolic feedback mechanism that 1) decreases hepatic glucose recycling via suppression of glucokinase expression in the basal state to preserve hepatic glucose production and 2) increases hepatic responsiveness in the fasted-to-fed transition. In *Pten*^{+/-} mice, hepatic gene expression of glucokinase was 10-fold less than wild-type (*Pten*^{+/+}) mice in the fasted state and reached *Pten*^{+/+} values in the fed state. Glucose-6-phosphatase expression was the same for *Pten*^{+/-} and *Pten*^{+/+} mice in the fasted state, and its expression for *Pten*^{+/-} was 25% of *Pten*^{+/+} in the fed state. This study demonstrates how intra- and interorgan flux compensations can preserve glucose homeostasis (despite a specific gene defect that accelerates glucose disposal) and how flux phenotyping can dissect these tissue-specific flux compensations in mice presenting with a “silent” phenotype. *Diabetes* 55: 3372–3380, 2006

From the ¹Department of Medicine, State University of New York at Stony Brook, Stony Brook, New York; ²Regeneron Pharmaceuticals, Tarrytown, New York; the ³Department of Pathology, University of California Los Angeles, Los Angeles, California; the ⁴Department of Pediatrics, Harbor-University of California Los Angeles Biomedical Institute, Torrance, California; the ⁵Department of Preventive Medicine, State University of New York at Stony Brook, Stony Brook, New York; the ⁶Molecular Biology Institute, University of California Los Angeles, Los Angeles, California; and the ⁷Departments of Pharmacological Sciences and Physiology and Biophysics, State University of New York at Stony Brook, Stony Brook, New York.

Address correspondence and reprint requests to Irwin J. Kurland, SUNY at Stony Brook, HSC T-15 Room 060, Stony Brook, NY 11794-8154. E-mail: irwin.kurland@stonybrook.edu.

Received for publication 2 January 2006 and accepted in revised form 6 September 2006.

Additional information for this article can be found in an online appendix at <http://diabetes.diabetesjournals.org>.

AUC, area under the curve; G6PDH, glucose-6-phosphate dehydrogenase; GC/MS, gas chromatography–mass spectrometry; glucose-6-P, glucose-6-phosphate; HGP, hepatic glucose production; HR-dGTT, hepatic recycling deuterated glucose tolerance test; HR-GTT, hepatic recycling glucose tolerance test; ipGTT, intraperitoneal glucose tolerance test; IIT, insulin tolerance test; PI3-K, phosphatidylinositol 3-kinase; PPAR, peroxisome proliferator-activated receptor; PTEN, phosphatase and tensin homolog deleted on chromosome 10; TCA, trichloroacetic acid.

DOI: 10.2337/db06-0002

© 2006 by the American Diabetes Association.

The costs of publication of this article were defrayed in part by the payment of page charges. This article must therefore be hereby marked “advertisement” in accordance with 18 U.S.C. Section 1734 solely to indicate this fact.

Controversy still exists as to whether the liver is a primary site of insulin resistance or whether the hepatic response to maintain glucose homeostasis in the face of peripheral insulin resistance is primarily compensatory (1). Loss of the liver insulin receptor results in primary hepatic insulin resistance, marked by elevations in PEPCK and glucose-6-phosphatase expression, and decreased glucokinase expression (2,3). However, an acute loss of the liver insulin receptor, secondary to treatment with antisense oligonucleotides, resulted in hepatic insulin resistance with no change in hepatic glucose production (HGP), although the source of intrahepatic fluxes contributing to HGP (glycogenolysis versus gluconeogenesis) are altered in a compensatory fashion to preserve HGP (4).

Factors that directly regulate phosphatidylinositol content, in particular the phosphatase and tensin homolog deleted on chromosome 10 (PTEN), have shown the pathway to be a central pathway in glucose metabolism (5,6), as opposed to other modulators (7,8). Rodent studies using *Pten* antisense oligonucleotides in *ob/ob* and *db/db* mice also suggest that a reduction of PTEN function, primarily in liver (and to a lesser degree in fat), is sufficient to impact the regulation of the whole-body glucose metabolic network in vivo (9). Recent experiments suggest that while the relative expression of *Pten* in different insulin-sensitive tissues is the major determinant in the modulation of glucose homeostasis, the effect seen is tissue dependent. Specifically, with *Pten* deletion in skeletal muscle, the metabolic effects are “silent” in standard diet-fed animals but are sufficient to prevent diet-induced obesity and insulin resistance (10). Kushner et al. (11) reported that wild-type mice and *Pten*^{+/-} mice have essentially similar responses to an insulin tolerance test (ITT) and glucose tolerance test. In contrast, adipose-specific *Pten* deletion resulted in improved systemic glucose tolerance and insulin sensitivity (12). Mice with a hepatic-specific *Pten* deletion also show increased insulin sensitivity and glucose disposal (13,14). However, as opposed to the muscle- or adipose-specific *Pten* deletion models, this was accompanied by progressive steatosis, dramatically increased liver weight, and a reduction in peripheral fat stores (13,14). The disparity between the whole-body *Pten*-deficient mouse and the tissue-specific *Pten*^{-/-} phenotypes suggests that the metabolic profile found for each tissue-specific mouse model is an accentu-

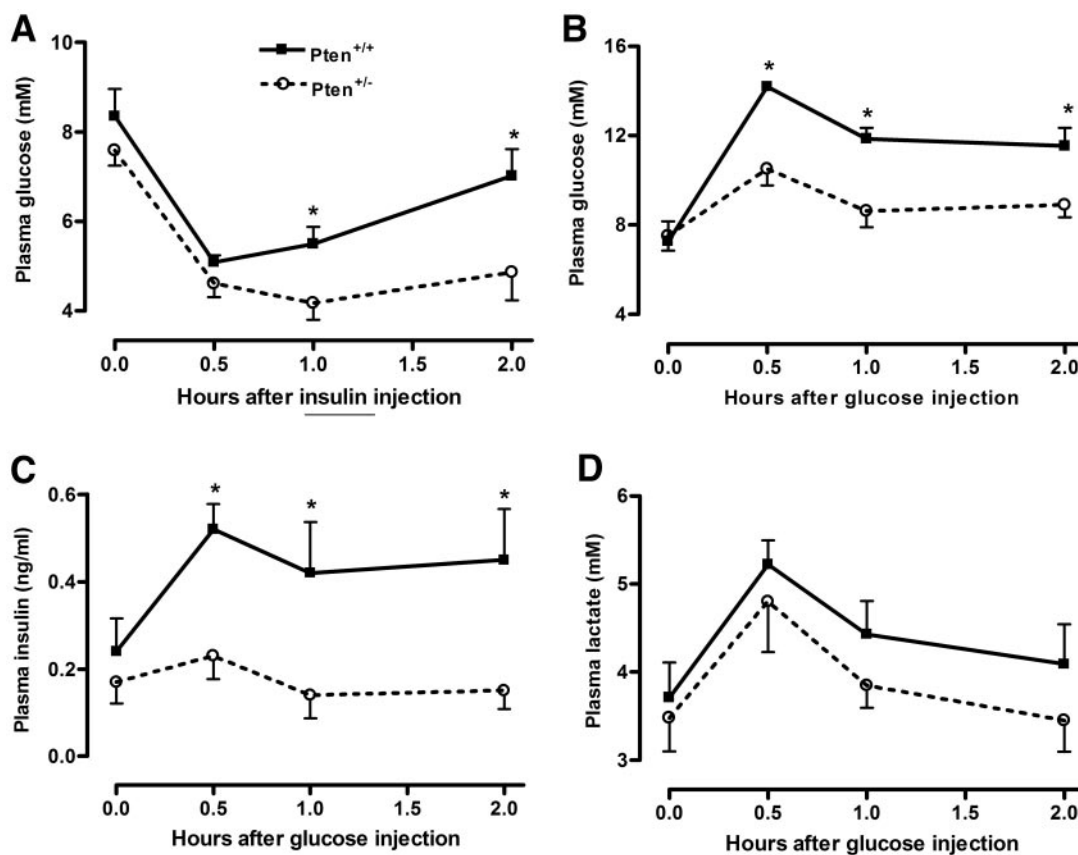


FIG. 1. Standard provocative insulin and glucose tolerance tests. Intraperitoneal ITT response for *Pten*^{+/+} and *Pten*^{+/-} mice (A). The ITT (0.75 unit/kg) was performed on *Pten*^{+/+} littermate control ($n = 10$) and *Pten*^{+/-} ($n = 7$) mice after a 4-h fast (see RESEARCH DESIGN AND METHODS). Time course of plasma glucose (B), insulin (C), and lactate (D) in response to a 1-mg [1,2-¹³C₂]glucose per g body wt ipGTT. The ipGTT was performed on *Pten*^{+/+} ($n = 5$) and *Pten*^{+/-} ($n = 7$) mice after a 15-h overnight fast. All data are presented as means \pm SE. * $P < 0.05$ between *Pten*^{+/+} and *Pten*^{+/-} mice, determined by Student's t test.

ation, or diminishment, of the effect of PTEN deficiency for a particular insulin-sensitive tissue and that compensatory mechanisms may result in detection of a seemingly “silent” phenotype.

The purpose of this study was to address the disparities in the tissue-specific insulin action of *Pten* heterodeficient mice by using stable isotope flux phenotyping (15–17) to determine compensatory flux mechanisms that preserve glucose homeostasis in the whole-body *Pten*^{+/-} mouse. This approach applied to the peroxisome proliferator-activated receptor (PPAR) α knockout (KO) mice showed increased peripheral glucose disposal observed in the fasted and fed states, along with increased total HGP, facilitated by a compensatory mechanism that reduced intrahepatic “futile” glucose/glucose-6-phosphate (glucose-6-P) recycling, allowing HGP to be maximal with the “futile” wasting of intracellular ATP minimized (17). This led us to hypothesize that perhaps compensatory interactions between hepatic glucose flux recycling and peripheral glucose disposal may help maintain glucose homeostasis, in general, when peripheral glucose disposal is affected.

Utilizing this approach in *Pten*^{+/-} mice, we clearly show an increase in peripheral glucose disposal and a decrease in glucose/glucose-6-P recycling, which we believe is the primary hepatic compensatory mechanism for maintaining HGP sufficient for supplying the increased peripheral disposal of glucose in this whole-body *Pten*^{+/-} mouse model. This result indicates the presence of compensatory

mechanisms underlying the homeostatic response to disorders in phosphatidylinositol 3-kinase (PI3-K)-mediated regulation. Gain of function, seen as increased peripheral glucose disposal in the *Pten*^{+/-} mice, by a reduction in whole-body PTEN levels, results in compensation by a metabolic feedback mechanism that decreases hepatic glucose recycling via suppression of glucokinase expression in the basal state. The basal hepatic effect is a loss of function, or responsiveness, to elevated PI3-K pathway activity. Increased hepatic responsiveness to *Pten* deficiency was seen for glucokinase for the fasted-to-fed transition, indicating that compensatory feedback mechanisms are adaptive for the metabolic state. Compensations seen for the whole-body *Pten*^{+/-} may be altered, or absent, in muscle-, adipose-, or liver-specific *Pten*-deleted mice. For example, steatosis was evident in the liver-specific *Pten*-deleted mice (13,14), but we found it was not present in the *Pten*^{+/-} mice, despite evidence for increased hepatic insulin responsiveness. These data suggest it may be very useful to use metabolic network analyses, such as stable isotope flux phenotyping, to dissect tissue-specific insulin action in vivo in the context of whole-body deficiencies of insulin signaling effectors, rather than inferring metabolic actions from tissue-specific deletion models.

RESEARCH DESIGN AND METHODS

Whole-body *Pten*^{+/-} mice were used from two different colonies. The ITT (Fig. 1A) and baseline body composition/serum studies (supplementary Table 1 [available at <http://diabetes.diabetesjournals.org>]) were done on *Pten*^{+/-}

mice of 10–14 weeks of age derived by the lab of Ramon Parsons, as previously described (18), from a colony maintained at Regeneron. Also, these mice, at 6 months of age, were used for supplementary Fig. 1, which describes the characteristics of liver and adipose tissues of *Pten*^{+/-} mice. The derivation of the *Pten*^{+/-} mice for all the remaining experiments has been described previously (19), but these mice have not been used for similar studies of glucose homeostasis. This colony was maintained at the University of California Los Angeles, and male and female *Pten*^{+/+} or *Pten*^{+/-} mice were ranged from 14 to 18 weeks in age, with average body weight 27.1 ± 1.0 g for *Pten*^{+/+} mice and 24.8 ± 1.3 g for *Pten*^{+/-} mice ($P > 0.05$, Student's *t* test). There were no significant body weight differences between male and female mice, either in *Pten*^{+/+} or *Pten*^{+/-} mice from this colony. All animals used in this study were tumor free in tissues examined at the time of killing. All animals were maintained under 12-h light/dark conditions and were fed standard laboratory chow diet. Animal studies were conducted in accordance with the IACUC guidelines and the protocol approved by the institutional review board.

Body composition was determined for each animal by dual-emission X-ray absorptiometry (PIXImus; General Electric Lunar, Madison, WI). Percent of lean mass and fat mass were calculated as a proportion of the total body weight of the animal. Ten *Pten*^{+/+} and 7 *Pten*^{+/-} males were examined at 10 weeks of age, while 7 *Pten*^{+/+} and 3 *Pten*^{+/-} females were examined at 11 weeks of age.

Indirect calorimetry. Metabolic parameters were measured using an Oxy-mas (Columbus Instruments, Columbus, OH) open-circuit indirect calorimetry system as previously described (20). Ten *Pten*^{+/+} and 7 *Pten*^{+/-} males were assessed at 12 weeks of age.

ITT. Following a 4-h morning fast, animals were bled from the tail for a baseline measurement. An insulin bolus was administered intraperitoneally at 0.75 units/kg body wt (R-insulin; Eli Lilly, Indianapolis, IN). Tail blood was sampled at 30, 60, and 120 min after insulin administration. Blood glucose was measured by the Bayer Ascensia DEX2 glucometer (Bayer Diagnostics, Tarrytown, NY). Ten *Pten*^{+/+} and 7 *Pten*^{+/-} males were examined at 11 weeks of age.

Biochemical/serum analysis. Serum samples were analyzed for cholesterol, aspartate aminotransferase, alanine aminotransferase, and alkaline phosphatase using the Bayer 1650 blood chemistry analyzer (Tarrytown, NY). Nonesterified free fatty acids were analyzed by a diagnostic kit (Wako, Richmond, VA). Serum was collected from 10 *Pten*^{+/+} and 7 *Pten*^{+/-} males and 7 *Pten*^{+/+} and 3 *Pten*^{+/-} females at 13 and 14 weeks of age, respectively. For the intraperitoneal glucose tolerance test (ipGTT) studies, plasma glucose and lactate concentrations were determined by COBAS MIRA analyzer (Roche Molecular Biochemicals) using reagents provided by Raichem (San Diego, CA). Glucose UV Reagent (catalog no. 80017) was used for glucose determinations; Stat-Pack Rapid Lactate test (catalog no. 869218) was used for lactate. Liver tissues taken from 18-h fasted mice were used to determine hepatic glycogen contents. Glucose residues derived from the liver tissues were prepared and determined as previously described (15). Plasma insulin was determined using an ultra-sensitive rat/mouse Insulin ELISA kit (catalog no. 90060; Crystal Chem).

HGP. Determination of HGP was carried out by constant infusion of [¹³C₆]glucose (99% enriched; Cambridge Isotope Laboratories, Andover, MA) through a miniosmotic pump (Alzet model 2001D; duration 24 h) (15). Four *Pten*^{+/+} and four *Pten*^{+/-} males were examined at 16–18 weeks of age. Briefly, fasting of animals was initiated at 4 P.M., and a miniosmotic pump containing 0.25 mg/μl [¹³C₆]glucose was quickly inserted to subcutaneous space of the animal at 7 P.M. under ~5% isoflurane. Blood samples were collected by orbital bleeding at 10 A.M. the next morning. HGP rate was determined using the following equation: HGP (in milligrams per kilogram body weight per minute) = infusion rate × (1/*E*_{Tracer} - 1). The infusion rate (in milligrams per kilograms per minute) = miniosmotic pump rate (8 μl/h calibrated by the manufacturer) × [¹³C₆]glucose concentration (0.25 mg/μl mouse body wt [kg]). *E*_{Tracer} is the enrichment of plasma [¹³C₆]glucose determined by gas chromatography-mass spectrometry (GC/MS) analysis. GC/MS conditions, sample preparations for GC/MS analysis, and a detailed description of equations and calculations for HGP can be found in our previous study (15).

Glycerol production and HGP from substrate glycerol. Four *Pten*^{+/+} and four *Pten*^{+/-} males at 16–18 weeks of age were used to determine glycerol production and HGP from glycerol, as previously described (15). Briefly, fasting of animals was initiated at 4 P.M., and a miniosmotic pump containing 0.3 mg/μl [¹³C]glycerol was quickly inserted to subcutaneous space of an animal at 7 P.M. under ~5% isoflurane. Blood samples were collected by orbital bleeding at 10 A.M. the next morning and 5 h after refeeding. Similar to HGP described above, glycerol production rate (in milligrams per kilograms body weight per minute) = infusion rate × (1/*E*_{Tracer} - 1). The infusion rate (in milligrams per kilograms per minute) = miniosmotic pump rate (8 μl/h

calibrated by the manufacturer) × [¹³C]glycerol concentration (0.3 mg/μl mouse body wt [kg]). *E*_{Tracer} is the enrichment of plasma [¹³C]glycerol determined by GC/MS analysis.

HGP from substrate glycerol was determined using the following equations: HGP from glycerol (in milligrams per kilograms per minute) = (glycerol production rate) × (glycerol FRC), where FRC is the fractional contribution of glycerol to hepatic glucose synthesis. Glycerol FRC = (M1/2m1) + (M2/m1), where M1 is the enrichment of plasma ¹³C-glucose and M2 the enrichment of plasma ¹³C₂-glucose, which were synthesized from infused [¹³C]glycerol, and m1 is the enrichment of plasma [¹³C]glycerol. The enrichments of plasma M1 and M2 glucose, as well as plasma m1 glycerol, were determined by GC/MS (15).

The intraperitoneal hepatic recycling glucose tolerance tests. Mice were fasted at 7 P.M. and insulin or glucose injected intraperitoneally at 10 A.M. the next morning. Each point of the hepatic recycling glucose tolerance test (HR-GTT) was the average of five male *Pten*^{+/+} or seven *Pten*^{+/-} mice (five males and two females), with average age of 14 weeks. Blood samples for insulin and glucose analysis were collected at various time points as indicated in Fig. 1 (see RESULTS). [²H]glucose and [6,6-²H₂]glucose were >98% enriched and sterility/pyrogenicity tested by the manufacturer (Cambridge Isotope Laboratories). Ten *Pten*^{+/+} and 14 *Pten*^{+/-} male mice were used in these tests.

In the hepatic recycling deuterated glucose tolerance test (HR-dGTT), a mixture of [²H]glucose (0.5 mg/g body wt) and [6,6-²H₂]glucose (0.5 mg/g body wt) was used. During the HR-dGTT, hepatic uptake of [²H]glucose generally leads to the loss of deuterium label at the C2 position due to isomerization between glucose-6-P and fructose-6-phosphate. As reviewed by Wolfe and Chinkes (21), hepatic glucose uptake of [6,6-²H₂]glucose generally leads to loss of the deuterium label, when 3-carbon pyruvate produced is converted to oxaloacetate and when malate is converted to fumarate. Also, [6,6-²H₂]glucose that is recycled back from fructose-1,6-bisphosphate back to glucose (without being broken down to 3-carbon precursors) will lose a deuterium atom. We found in our ipGTT studies that [6,6-²H₂]glucose did not significantly recirculate during the ipGTT by examining the formation of singly labeled [6-²H]glucose, which theoretically could be produced by recirculation of [6,6-²H₂]glucose, through monitoring for the C3-C6 EI fragment (data not shown). Therefore, we used the area under the curve (AUC) for [6,6-²H₂]glucose during the ipGTT to reflect the whole-body disposal of glucose.

When [²H]- and [6,6-²H₂]glucose are administered as a 1:1 mixture, the disappearance of the two isotopes [²H]- and [6,6-²H₂]glucose can be determined by mass fragmentography by assessing the M1 label in the C1-C4 fragment (for [²H]glucose) and the M2 label in the C3-C6 fragment (for [6,6-²H₂]glucose) of the electron-impact mass spectrometry. The difference between the two disappearance rates has long been recognized as the standard measure of futile cycling (i.e., glucose to glucose-6-phosphate and back [17,22,23]) and can be determined as: relative rate of glucose/glucose-6-P futile cycling = percent difference in plasma [²H]glucose vs. [6,6-²H₂]glucose = (percent [6,6-²H₂]glucose - percent [²H]glucose)/(percent [6,6-²H₂]glucose). GC/MS analyses of plasma glucose isotopomers during the HR-dGTT can be found in our previous study (17).

RNA quantitation. Total RNA was isolated from liver or skeletal muscle with Trizol (Invitrogen, Carlsbad, CA) and used as template for cDNA synthesis using oligo dT primers. Real-time PCR was performed with the iCycler iQ real-time detection system (BioRad, Hercules, CA) using SYBR Green PCR QuantiTect reagent (Qiagen, Valencia, CA). Each assay was performed in triplicate using 25–50 ng cDNA. In addition, a standard curve of four serial dilution points of control cDNA (ranging from 100 ng to 100 pg), as well as a no-template control, were included in each assay. The relative concentration of genes of interest was determined by plotting the threshold cycle (*C*_t) versus the log of the serial dilution points and normalizing to expression levels of an endogenous control gene, *TBP* (TATA box binding protein). Primer sequences used for real-time PCR were: glucokinase, forward 5'-TAT GAA GAC CGC CAA TGT GA-3', reverse 5'-TTT CCG CCA ATG ATC TTT TC-3'; glucose-6-phosphatase p36 subunit, forward 5'-CTG TGA GAC TGG ACC AGG GAG-3', reverse 5'-TTC CAC GAA AGA TAG CGA GAG-3'; glucose-6-phosphate dehydrogenase (G6PDH), forward 5'-GCT GGA TCT AAC TTA TGG CAA CA-3', reverse 5'-CGG ACA AAG TGC ATC TGG C-3'; and PEPCK, forward 5'-CAG CTG CTG CAG AAC ACA AGG-3', reverse 5'-GCT AAC TGC TAC AGC TAA CGT G-3'.

Statistical analyses. All data were expressed as means ± SE, except for data in Table 1, in which AUC was presented as means ± SD. Analyses for the significance of differences were performed using Student's *t* test or two-way ANOVA. The percent difference between the plasma [²H]- and [6,6-²H₂]glucose enrichments against time, during the ipGTT, was determined using linear regression analysis.

TABLE 1

Whole-body glucose disappearance and insulin sensitivity in *Pten*^{+/+} and *Pten*^{+/-} mice

Animals	AUC		
	Total glucose (mmol/l × h)	2 × M2 glucose (mmol/l × h)	Plasma insulin (ng × h/ml)
<i>Pten</i> ^{+/+}	23.59 ± 1.2	3.49 ± 0.12	0.86 ± 0.04
<i>Pten</i> ^{+/-}	18.04 ± 1.5*	2.22 ± 0.10*	0.33 ± 0.01*

Data are means ± SE. AUC for plasma glucose, [6,6-²H₂]glucose (M2), and insulin are compared between *Pten*^{+/+} and *Pten*^{+/-} mice during the 2-h time course of the HR-dGTT (1 mg/g body wt). M2 glucose reflects plasma glucose containing two deuterium atoms for the [6,6-²H₂]glucose ipGTT. M2 AUC is multiplied by 2 to calculate glucose disposal, as the glucose injected was only 50% M2 (see research design and methods). **P* < 0.05 between *Pten*^{+/+} and *Pten*^{+/-} mice, by Student's *t* test.

RESULTS

***Pten*^{+/-} mice exhibit enhanced whole-body glucose utilization and insulin sensitivity.** Analysis of a 0.75 units/kg body wt ITT, and the standard 1 mg/g body wt ipGTT, are shown in Fig. 1, as well as plasma insulin and lactate measurements during the ipGTT. Analysis of blood glucose levels revealed that there was no difference in either nonfasting (Fig. 1A) or fasting (Fig. 1B) values between the *Pten*^{+/+} and *Pten*^{+/-} mice. After challenge with a 0.75 units/kg bolus of insulin in the ITT, *Pten*^{+/-} mice clearly had lower plasma glucose at 1 and 2 h (Fig. 1A). Figure 1 also showed that plasma glucose and insulin levels, but not plasma lactate levels, were consistently lower for the *Pten*^{+/-} compared with *Pten*^{+/+} mice during the ipGTT (Fig. 1B–D).

To further characterize the increased insulin sensitivity in the *Pten*^{+/-} mice, we determined the AUC of plasma insulin, total plasma glucose (Table 1) during the time course of a stable isotope-labeled ipGTT, which we have termed the HR-dGTT (see RESEARCH DESIGN AND METHODS). In response to the same glucose load, *Pten*^{+/-} mice had a decrease of 65% in the insulin AUC compared with *Pten*^{+/+} mice but a 25% decrease in the total glucose AUC, which indicates accelerated glucose disposal in *Pten*^{+/-} mice.

Analysis of muscle glycogen levels in the fasted and fed states and the energy substrate utilization as assessed by indirect calorimetry were comparable between both *Pten*^{+/-} and *Pten*^{+/+} mice (data not shown). Since the muscle mass is by far larger than the liver or fat mass, the 25% decrease in the total glucose AUC may be due to accelerated glucose disposal, despite the lower insulin AUC during the HR-dGTT and/or a lower value of HGP in the *Pten*^{+/-} mice. To determine whether the decrease in the total glucose AUC can largely be attributed to increased muscle glucose uptake as a consequence of the muscle-specific actions of *Pten* heterodeficiency (or a decrease in HGP), we used the stable isotope flux phenotyping methodology.

Glucose disposal, futile cycling, and HGP in *Pten*^{+/-} mice. Although the ITT shows the predicted enhancement of insulin sensitivity with deletion of a single copy of *Pten*, it gives little information about peripheral glucose uptake and/or hepatic insulin action. To determine this, we assessed plasma glucose disposal during the HR-dGTT, a 1 mg/g body wt ipGTT that uses a glucose bolus composed of equal amounts of the deuterium-labeled stable isotopes [2-²H]glucose and [6,6-²H₂]glucose (17,22). The plasma [6,6-²H₂]glucose (M2) glucose isotopomer injected was

quantitated by GC/MS (see RESEARCH DESIGN AND METHODS). Mass spectrometric quantitation of plasma M2 glucose reveals that *Pten*^{+/-} mice have an accelerated rate of glucose disposal into peripheral tissues (Fig. 2A). The M2 AUC for the *Pten*^{+/-} mice was approximately half that of *Pten*^{+/+} mice, reflecting a dramatic acceleration of the disposal of the administered glucose when PTEN is deficient (Table 1).

Given that the HR-dGTT revealed increased peripheral (mainly muscle) glucose uptake and insulin sensitivity, how can the compensations that preserve glucose homeostasis be best assessed in vivo? Fasting glucose levels are equal for *Pten*^{+/+} and *Pten*^{+/-} mice, suggesting mechanism(s) exist for matching peripheral glucose utilization to HGP. Intra-HGP or utilization is a function of the degree, and net direction, of glucose recycling through the three “futile” or substrate cycles that govern net glycolysis/gluconeogenesis. Also, whether the liver is storing or releasing glucose to and from glycogen affects the mass of carbon in the glucose-6-P pool. These “futile” cycles are the glucose/glucose-6-P, fructose/fructose-6-P, and phosphoenolpyruvate/pyruvate substrate cycles. The amount of glycogen stored in the liver in transition between the fasted and fed states would be dependent on the degree of plasma insulin and glucose excursions in response to a meal or glucose load, as well as the route taken within the liver for recycling/metabolizing glucose. The HR-dGTT is designed to examine at what level intrahepatic futile recycling of glucose may be affected.

Hepatic glucose cycling at the level of glucose/glucose-6-P is known as glucose futile cycling and is traditionally determined using separate infusions of [2-³H]glucose and [6-³H]glucose tracers (23). The infusion of [2-³H]glucose is known to provide a different estimate of glucose turnover rate than that from the infusion of [6-³H]glucose (23). The difference is attributed to the fact that the hydrogen in the carbon-2 position of glucose is lost in the equilibrium reaction of isomerization of glucose-6-P to fructose-6-P, whereas the hydrogen in the carbon-6 position is retained (Fig. 2C). The difference between the plasma enrichments of the [2-²H]glucose and [6,6-²H₂]glucose during the HR-dGTT can be used here to estimate glucose/glucose-6-P cycling. Figure 2B shows that at all times during the HR-dGTT, the percent difference between the plasma enrichments of the two tracers is greater for the *Pten*^{+/+} than for the *Pten*^{+/-} mouse, indicating less glucose/glucose-6-P futile cycling for the *Pten*^{+/-} mice. In separate experiments, total HGP was measured by the constant infusion of [U-¹³C₆]glucose via an Alza osmotic mini-pump. As shown in Fig. 3A, there is no difference in total HGP between *Pten*^{+/-} and *Pten*^{+/+} mice in the 18-h fasted state. Since the net glucose/glucose-6-P flux equals HGP (Fig. 2C), an increased peripheral glucose disposal and decreased hepatic glucose recycling may play compensatory roles to maintain glucose homeostasis in *Pten*^{+/-} mice. The increase in peripheral glucose uptake may be a direct and unavoidable consequence of increased PI3-K action due to PTEN deficiency. The decrease in glucose/glucose-6-P recycling preserves HGP, despite the known action of PI3-K signaling, to increase glucokinase expression and decrease glucose-6-phosphatase expression (24–26). This suggests that hepatic glucose recycling is modulated by an undetermined in vivo mechanism to compensate for peripheral glucose disposal, in order to preserve glucose homeostasis. It may be that measurements of glucose/glucose-6-P recycling via HR-dGTT are more sensitive than

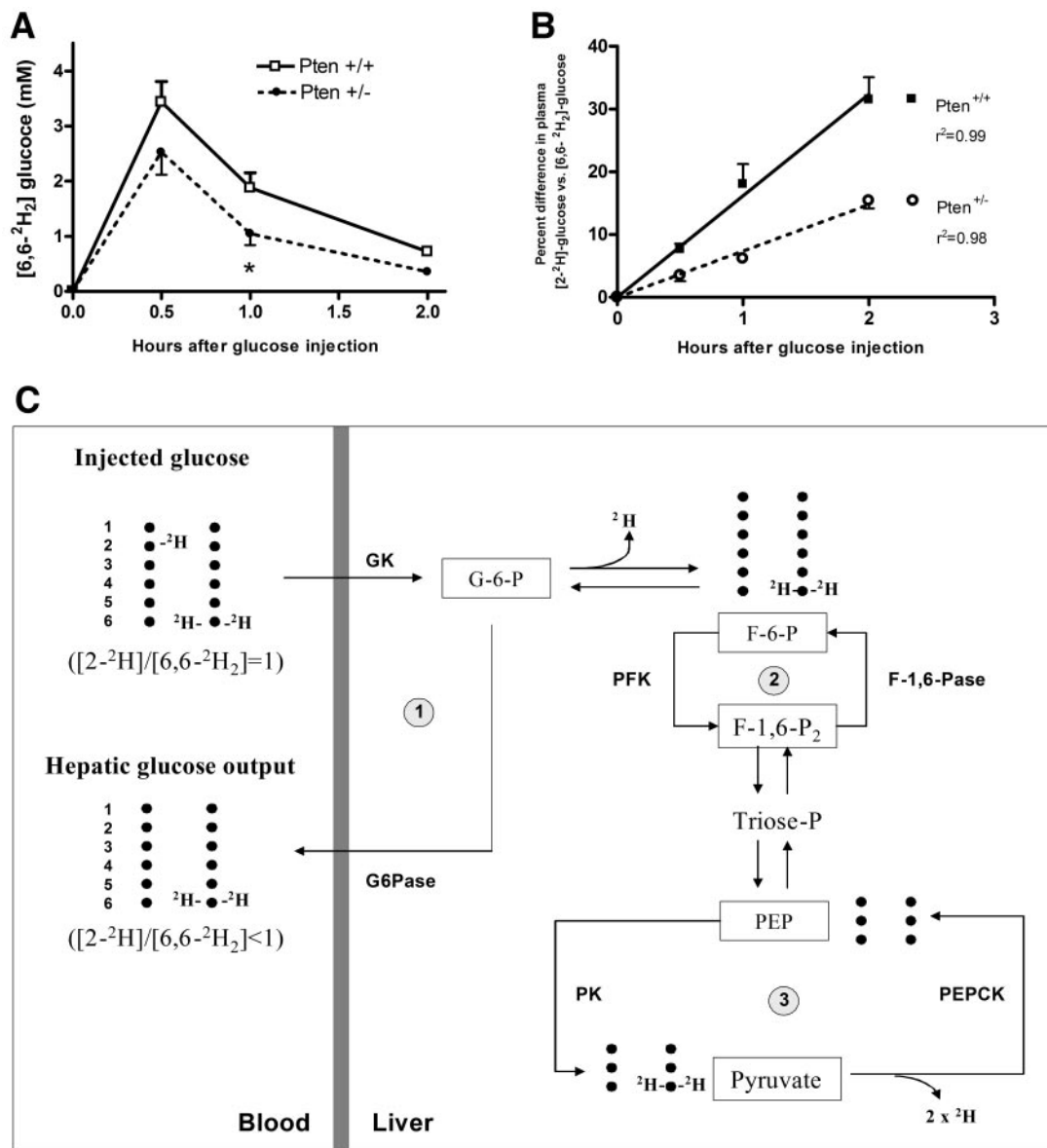


FIG. 2. A: The HR-dGTT. *Top panel:* Time course of the [6,6-²H₂]glucose (M2) isotopomers using 1 mg/g body wt of a 1:1 mixture of [2-²H]- and [6,6-²H₂]glucose for the ipGTT. Data are presented as means \pm SE. **P* < 0.05 between *Pten*^{+/+} and *Pten*^{+/-} mice, determined by Student's *t* test. M2 glucose levels are significantly lower for *Pten*^{+/-} versus *Pten*^{+/+} mice, suggesting increased peripheral disposal of glucose for the *Pten*^{+/-} mice. *B:* Time course of the percent difference between the plasma [2-²H]- and [6,6-²H₂] glucose enrichments during the deuterated glucose HR-dGTT. The HR-dGTT was performed using 1 mg/g body wt of a 1:1 mixture of [2-²H]- and [6,6-²H₂]glucose on *Pten*^{+/-} (*n* = 5) and *Pten*^{+/+} (*n* = 7) mice after a 15-h overnight fast. The data are presented as means \pm SE. The percent difference between the plasma enrichments of the two tracers reflects the relative rate of de-deuteration of [2-²H]- versus [6,6-²H₂]glucose, which is a measure of net hepatic glucose phosphorylation or, equivalently, glucose/glucose-6-P futile cycling. At all time points during the IPGTT, the percent difference between the plasma enrichments of the two tracers is greater for the *Pten*^{+/+} than for the *Pten*^{+/-} mouse, indicating a much smaller amount of glucose/glucose-6-P futile cycling for the *Pten*^{+/-} mice. The slope is 16.2 \pm 0.53% for the *Pten*^{+/+} mice versus 7.4 \pm 0.35% for *Pten*^{+/-} mice. *C:* Illustrative diagram of pathways for hepatic metabolism of the deuterium-labeled [2-²H₁]/[6,6-²H₂]glucose. De-deuteration of [2-²H₁]glucose occurs during the equilibration of glucose-6-P (G-6-P) with fructose-6-P (F-6-P), which is theoretically two orders of magnitude faster than any other glycolytic or gluconeogenic flux. De-deuteration of [6,6-²H₁]glucose does not occur until the deuterated glucose reaches the level of pyruvate. F-1,6-P₂, fructose-1,6-bisphosphate; GK, glucokinase; G6Pase, glucose-6-phosphatase; PK, pyruvate kinase.

HGP in detecting the hepatic effects of PI3-K action, since it is the flux difference in the glyconeogenic versus glycolytic arms of the glucose/glucose-6-P cycle that helps to determine HGP. For this reason, we then sought to examine relevant hepatic characteristics governing HGP.

Hepatic characteristics governing HGP are altered in *Pten*^{+/-} mice. Discrepancies in the measurement of HGP can occur due to differences in fasting insulin levels, the amount of hepatic glycogen, and the expression level of gluconeogenic enzymes. Fasting insulin levels were not significantly different between *Pten*^{+/-} and *Pten*^{+/+} mice

in these experiments (Fig. 1C), as opposed to the decreased fasting insulin levels seen for the adipose-specific deletion of *Pten* (aP2-*Pten*^{+/-} [12]) and the liver-specific deletion of *Pten* (Alb-*Pten*^{+/-} [13,14]). Figure 3A also shows that while the fasted levels of hepatic glycogen are twofold higher, the fed levels are one-third less for *Pten*^{+/-} mice than for *Pten*^{+/+} littermates. This may indicate that PTEN deficiency facilitates the retention of hepatic glycogen via increasing hepatic insulin action in the basal state.

The expression of glucokinase and glucose-6-phosphatase, two enzymes that control the glucose/glucose-6-P

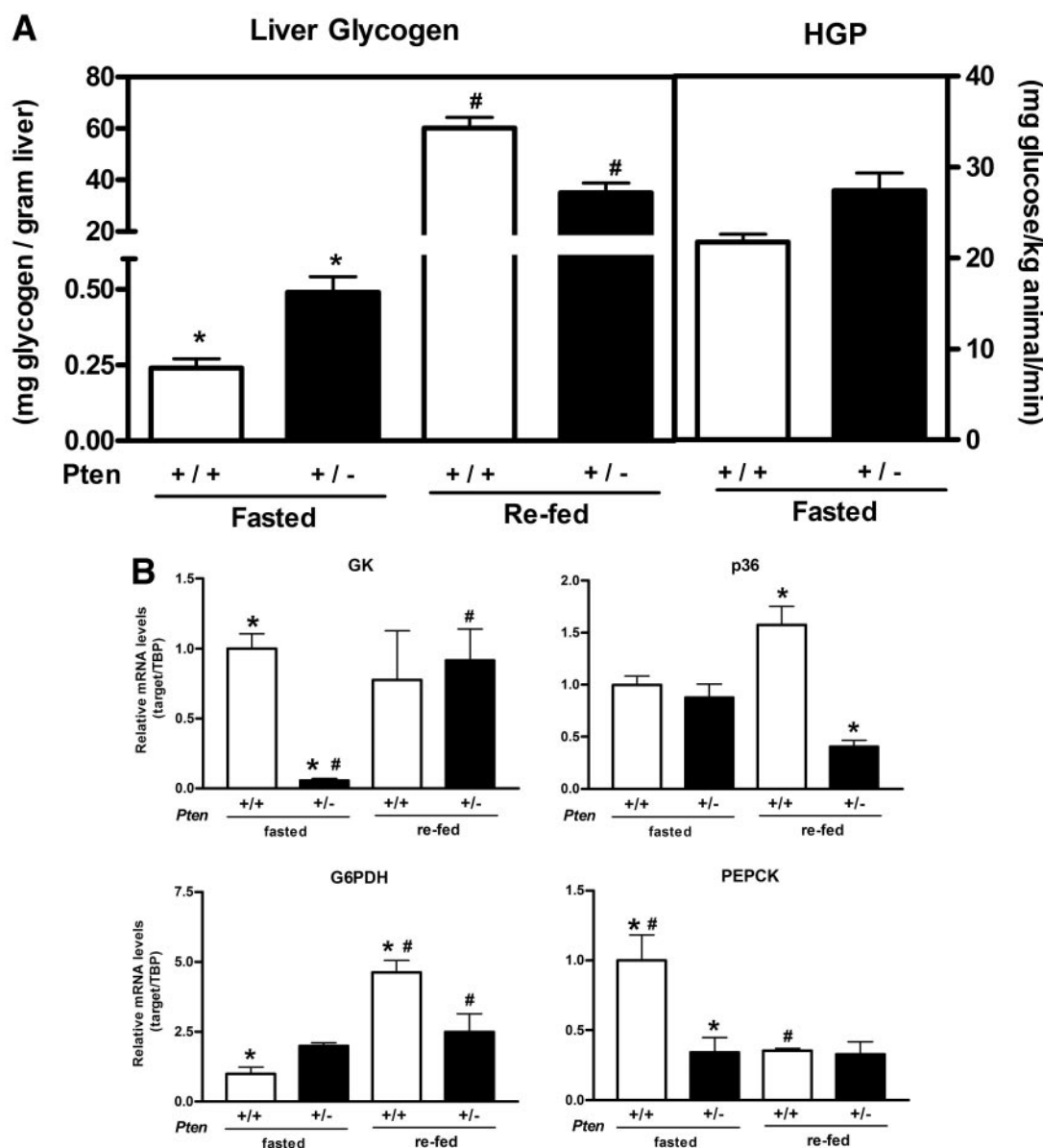


FIG. 3. Hepatic glycogen content and HGP in the $Pten^{+/+}$ and $Pten^{+/-}$ mice (A). Liver glycogen was measured from animals ($n = 4$ for each group) after 18 h overnight fasting or animals ($n = 4$ for each group) after 18 h fasting, followed by a 5-h refeeding. HGP was determined in 18-h fasted mice, which were constantly infused with [$^{13}\text{C}_6$]glucose, administered by subcutaneously inserted Alza miniosmotic pumps. * $P < 0.05$ for $Pten^{+/+}$, # $P < 0.05$ for $Pten^{+/-}$ mice, as determined by Student's t test. Hepatic gene expression in the $Pten^{+/+}$ and $Pten^{+/-}$ mice determined by RT-PCR (B). Tissues for this gene expression study were taken either from 18-h fasted mice ($n = 4$ for each group) or from mice first fasted 18 h then re-fed standard chow for 5 h ($n = 4$ for each group). Both $Pten^{+/+}$ and $Pten^{+/-}$ mice consumed similar amount of regular chow during the 5-h refeeding period (data not shown). $P < 0.05$ by two-way ANOVA, followed by Bonferroni's post tests. Statistical differences determined by Bonferroni's post tests of multiple comparison are shown as * $P < 0.05$ between the fasted $Pten^{+/+}$ and $Pten^{+/-}$ mice or # $P < 0.05$ between the re-fed $Pten^{+/+}$ and $Pten^{+/-}$ mice. Two-way ANOVA indicated that both glucokinase (GK) and glucose-6-phosphatase (G6Pase) gene expression were significantly different for genotype/feeding interactions; G6PDH expression was different for both feeding status and genotype/feeding interactions; and PEPCK expression was different for genotype, feeding status, and their interactions. p36, catalytic subunit of glucose-6-phosphatase.

cycle, are heavily and oppositely regulated by insulin/PI3-K signaling by different transcription factors (24–26). Figure 3B shows that glucokinase expression in the 18-h fasted state of the $Pten^{+/-}$ mice is 10-fold less than that of $Pten^{+/+}$ mice. However, glucokinase is rapidly induced when moving from the fasted to the fed state. After 5 h of refeeding, $Pten^{+/-}$ mice glucokinase levels are equivalent to that of fed $Pten^{+/+}$ mice. This represents an important measure of increased hepatic responsiveness to insulin action, which is often overlooked. The expression of the catalytic subunit (p36) of glucose-6-phosphatase also shows a dynamic response to fasting. As opposed to

glucokinase, there is no difference in the expression levels of p36 glucose-6-phosphatase between the $Pten^{+/+}$ and the $Pten^{+/-}$ mice in the fasted state. However, p36 glucose-6-phosphatase expression is 75% less for $Pten^{+/-}$ mice in the fed state. These results suggest that PI3-K action alone is not the only factor regulating glucokinase expression and activity in the fasted state and in the fasted-to-fed transition. Rather, hepatic glucokinase expression is sensitive to the requirements of whole-body glucose homeostasis and is part of a compensatory mechanism for matching HGP to peripheral glucose demands.

There may also be a differential sensitivity for PTEN

facilitation of hepatic insulin action on the enzymes of the glyconeogenic, glycolytic, and pentose phosphate pathways in order to best adapt net HGP to peripheral glucose needs. As seen from Fig. 3B, the expression of enzymes in these pathways are affected differently for *Pten*^{+/+} versus *Pten*^{+/-} mice, in either the fasted and/or fed states. PEPCK seems more sensitive in the fasted state, while glucose-6-phosphatase seems more sensitive in the fed state to the heterodeficiency of *Pten*. Note that the decrease seen for PEPCK expression in the fasted state of the *Pten*^{+/-} mouse, to ~30% of basal expression, is not sufficient to restrict hepatic gluconeogenesis. At the beginning of the fasted-to-fed transition, the decreased glucose/glucose-6-P cycling in the *Pten*^{+/-} mice may just serve as a mechanism to maintain HGP to meet the peripheral glucose need, as flux through PEPCK is poised to decrease at this time. For livers isolated from liver-specific cytosolic PEPCK-null mice models, having either 0, 5, or 10% residual PEPCK expression, Burgess et al. (27) report that loss of the majority of PEPCK expression, leaving 10% residual PEPCK, resulted in only an ~20% decrease in gluconeogenesis from trichloroacetic acid (TCA) cycle intermediates. However, no appreciable gluconeogenic flux from TCA cycle intermediates was measured when there was zero residual PEPCK expression (27). It has been shown that complete ablation of PEPCK in liver-specific (28) or whole-body KO (29) mice results in a build-up of TCA cycle intermediates and a decrease in the rate of TCA cycle flux. This indicates that PEPCK has an important role in the removal of TCA cycle anions (cataplerosis) in general, just that this can be accomplished with very low levels of PEPCK expression. G6PDH expression is unaffected by *Pten* heterodeficiency in the fasted state but is decreased in the fed state, which may be part of a mechanism, along with the low glucokinase expression, restricting hepatic steatosis. The low glucokinase expression also allows HGP to be maximized in the *Pten*^{+/-} mouse, despite increased hepatic insulin sensitivity. These findings may also then support the existence of compensatory mechanisms that adapt liver glucose flux in specific metabolic pathways, not only for the regulation of hepatic glucose and lipid metabolism but also to best match HGP to peripheral glucose needs.

***Pten*^{+/-} mice exhibit only subtle changes in body composition and serum parameters.** A stable isotope flux phenotyping approach, utilizing [2-¹³C]glycerol, was used for the in vivo assessment of the endogenous rate of lipolysis. Lipolysis can be assessed by measurements of glycerol turnover, since 80–90% of glycerol production is derived from adipose tissue lipolysis (21,30,31), and this was not affected in *Pten*^{+/-} mice. Both in the 18-h fasted and 5-h re-fed states, there was no difference in the rate of glycerol production or HGP from glycerol between the *Pten*^{+/+} and *Pten*^{+/-} mice (Fig. 4). In light of the fasted/fed enzyme expression data, the HGP from glycerol data implies glucokinase flux has dramatically increased compared with glucose-6-phosphatase flux. Indeed, the 22% decrease in HGP from glycerol in the fed state between *Pten*^{+/-} and wild-type mice is borderline significant ($P = 0.05$), which could reflect the decreased expression of glucose-6-phosphatase and the similar expression of glucokinase, for *Pten*^{+/-} relative to wild-type mice in the fed state, due to the 10-fold induction of glucokinase for the whole-body *Pten*^{+/-} mouse in the fasted to fed transition.

The similar result seen for lipolysis for the *Pten*^{+/+} and *Pten*^{+/-} mice are consistent with body composition of

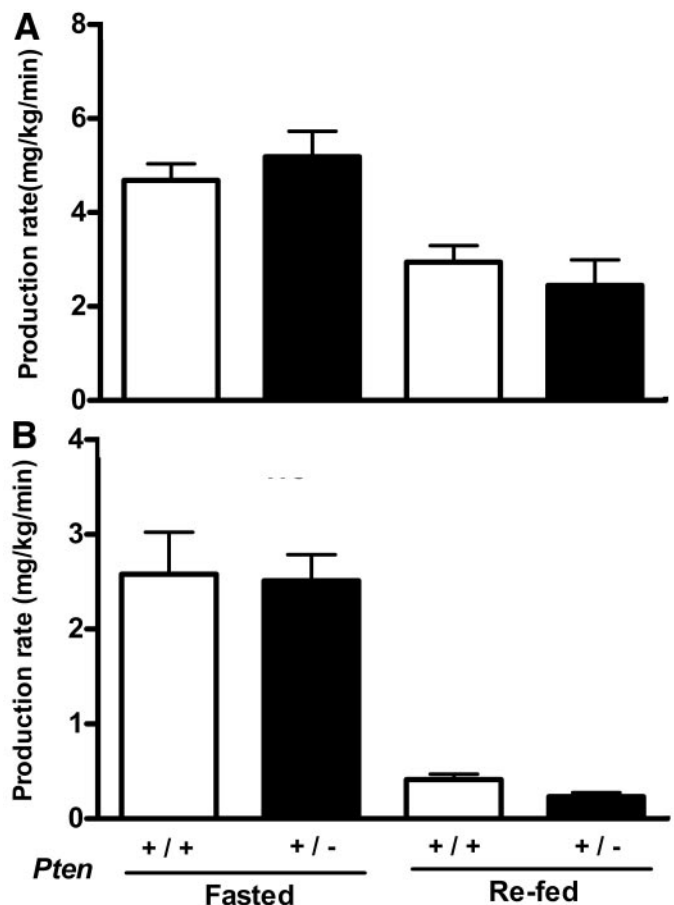


FIG. 4. Lipolysis and HGP from glycerol measurements. Glycerol production (A) rate and HGP from glycerol (B). Both were measured from 18-h fasted mice ($n = 4$) or mice fasted for 18 h and then re-fed standard chow for 5 h ($n = 4$) during a constant infusion of [2-¹³C]glycerol given via subcutaneously inserted mini-osmotic pumps. There were no differences observed in glycerol production and HGP from glycerol between the *Pten*^{+/+} and *Pten*^{+/-} mice in each feeding status, determined by Student's *t* test.

standard diet-fed male and female *Pten*^{+/-} mice. Body composition studies were performed by dual-energy X-ray absorptiometry scanning (supplementary Table 1). For both males and females, no change was observed in the percent lean body mass, the percent fat mass, or the bone mineral content. The liver, white adipose tissue, and brown adipose tissue of 36-week-old *Pten*^{+/-} mice were the same in color and appearance, as well as in weights (normalized by body weights), as the *Pten*^{+/+} mice (supplementary Fig. 1). This indicates that hepatic steatosis is not evident in *Pten*^{+/-} mice, which is further supported by no changes in basal serum chemistries for aspartate aminotransferase, alanine aminotransferase, alkaline phosphatase, albumin, creatinine, total protein, calcium, magnesium, or urea (data not shown). Interestingly, a significant 20% decrease in nonesterified fatty acids was observed for the group of male *Pten*^{+/-} mice but not for females (supplementary Table 1).

DISCUSSION

We have demonstrated the existence of a unique compensatory mechanism by which the body regulates hepatic glucose/glucose-6-P cycling to satisfy the basal needs for glucose supply to the brain and other peripheral tissues. This compensatory mechanism results in suppression of

glucokinase expression in the liver in the basal state in order to maximize HGP. The detection of this compensatory hepatic glucose recycling mechanism was made possible through the development and use of our HR-dGTT (17,22), and understanding the underlying principles of the HR-dGTT is necessary in order to discuss the significance of this study's findings.

In the HR-dGTT, the deuterium from [2-²H]glucose is not released until the glucose reaches the glucose-6-P pool. An increased rate of exchange of deuterium from [2-²H]- versus [6,6-²H₂]glucose can only occur if there is liver uptake of glucose and phosphorylation by glucokinase. The HR-dGTT, under the conditions of this study, reflects mainly the *in vivo* action of hepatic glucokinase. Glucokinase expression is heavily dependent on hepatic PI3-K activity (24). The novelty of this test is that measurements of the differences between [2-²H]- versus [6,6-²H₂]glucose enrichments yields an estimate that reflects flux through hepatic glucokinase during the ipGTT. Glucokinase expression was 10-fold less than wild-type mice in the fasted state, while the level of glucose-6-phosphatase, which catalyzes the reconversion of glucose-6-phosphate back to glucose, was the same in the fasted state as the wild-type mice (Fig. 3). Glucose-6-phosphatase, under the conditions in this study, has more of a secondary role (almost that of a "relay" enzyme to recirculate glucose-6-phosphate), in comparison to the role of glucokinase. The low value of glucokinase expression in the fasted state is counter to what would be expected for an enzyme whose expression is dependent on PI3-K pathway activity (24) in a tissue in which insulin action is potentiated via the heterodeficiency of *Pten*.

A hypothesis for the whole-body compensatory response to PTEN deficiency is that since the brain consumes a considerable fraction of basal glucose production, which is insulin independent, there is a need for the fasting HGP to be similar for *Pten*^{+/+} and whole-body *Pten*^{+/-} mice. This suggests that unique hepatic glucose recycling mechanisms have been activated in the whole-body *Pten*^{+/-} mouse model to regulate HGP, which could allow HGP to be at the level needed for brain and basal energy requirements.

It also appears from the isotopic flux phenotyping of the whole-body *Pten*^{+/-} mouse model that the effect of increased peripheral, mainly muscle, glucose disposal due to PTEN deficiency is primary, and compensatory mechanism(s) are evident in the liver, such as decreased glucose/glucose-6-P recycling. These hepatic compensatory mechanism(s) affect the expression of enzymes, such as glucokinase, in a fashion to override the effect of the acceleration of PI3-K action; thus, HGP matches the peripheral glucose need. Steatosis is not evident in the whole-body *Pten*^{+/-} mouse model. This is in contrast to the metabolic defects seen for the *Alb-Pten*^{-/-} mice, where hepatic compensatory mechanisms seem absent or distorted and where the liver also appears to be a primary site for greatly increased insulin action. *Alb-Pten*^{-/-} mice were seen to have decreased fasting glucose (13,14), as well as severe and progressive steatosis, manifested by the dysregulation of key aspects of fat metabolism. It was postulated that for the *Alb-Pten*^{-/-} mice, enhanced insulin action in the liver resulted in the redistribution of body fat from adipose tissue to the liver, which, along with increased hepatic lipogenesis, made the liver the sacrificial organ to maintain blood glucose control and lean body mass (13). This is not the situation we have found for the

whole-body *Pten*^{+/-} mouse model. Rather, the lack of hepatic steatosis in the *Pten*^{+/-} mouse may be partially due to the restriction of hepatic glucose uptake, due to low glucokinase expression, and the diversion of glucose from liver to muscle for increased uptake. Lack of steatosis in the *Pten*^{+/-} mouse may also be partially due to the decreased G6PDH in the fed state, which would restrict the supply of NADPH for lipogenesis.

The whole-body *Pten*^{+/-} mouse model shows no change in lipolysis, as opposed to the altered rate of lipolysis noted by Stiles et al. (13) for the *Pten* liver-specific deletion. While liver glycogen is increased for the whole-body *Pten*^{+/-} mouse, this increase in liver glycogen is restricted to the fasted state, indicative of increased hepatic insulin action in the fasted state. However, the fed level of hepatic glycogen is decreased for the whole-body *Pten*^{+/-} mouse model, which, extrapolating from the ipGTT response, suggests that it is not merely potentiation of insulin signaling effector phosphorylation that determines the metabolic consequences of insulin action, but the integrated response of the metabolic network. There is less glycogen in the fed state because the *Pten*^{+/-} mouse has a decreased glucose excursion, relative to *Pten*^{+/+} mice, in the fasted-to-fed transition and, thus, less glucose is available to be stored.

The *Pten*^{+/-} mouse is a subtle metabolic phenotype, virtually "silent" by conventional testing, as standard ipGTTs used to evaluate this model may not detect any difference in plasma glucose concentration depending on the amount of glucose administered. For example, after completion of our studies, Kushner et al. (11) reported that wild-type and *Pten*^{+/-} mice displayed identical hypoglycemic responses to an ITT. However, they used 1.5 units/kg insulin, rather than the 0.75 units/kg insulin used in our study. Similar to our study, they also reported normal fasting glucose for ≥3-month-old *Pten*^{+/-} mice. However, they fail to see differences in glucose tolerance in response to a 2 mg/g ipGTT, which is evident in our studies using a 1 mg/g ipGTT. While a possible solution for improving the assessment capabilities of conventional ITT and ipGTT testing would be to do a dose response, this would require more time per animals, while the HR-dGTT yields definitive results on the presence of increased peripheral insulin sensitivity/increased glucose disposal (Table 1), as well as pin-pointing changes in hepatic glucose recycling. The advantages of the HR-dGTT over standard ipGTT/ITT testing in the ability to characterize a "silent" mouse model with increased insulin sensitivity at a crucial link in the insulin signaling pathway (*Pten*) has implications more far reaching than simply the description of a phenotype.

It can be postulated from this work that hepatic glucose/glucose-6-P futile cycling may play an important compensatory role for balancing changes in peripheral glucose disposal in order to maintain glucose homeostasis. As we previously demonstrated, PPARα KO mouse had increased peripheral glucose uptake, increased HGP, and decreased hepatic glucose/glucose-6-P cycling (15,17). Measurement of hepatic enzyme expressions showed that there was no difference in glucose-6-phosphatase mRNA levels between the wild-type and PPARα KO mice but that there were dramatic decreases in the mRNA levels of glucokinase and pyruvate kinase in the PPARα KO mice during the fast-to-fed transition, which served to minimize the wastage of ATP in "futile cycling" in order to maximize net HGP (15,17). Interestingly, it has been shown that increased glucose/glucose-6-P cycling occurs in type 2 diabetes,

where peripheral glucose disposal decreased and peripheral insulin resistance is increased (rev. in 22). A cause and effect relationship between glucose/glucose-6-P futile cycling and peripheral glucose disposal appears to be crucial for the maintenance of glucose homeostasis. Our further work will delineate the metabolic network mechanisms linking the regulation of hepatic glucose recycling to peripheral glucose disposal.

ACKNOWLEDGMENTS

This work was supported by a grant from the American Diabetes Association (to I.J.K.), National Institutes of Health (NIH) Grants DK58132-01-A2 (to I.J.K.) and DK56090-A1 (to W.N.P.L.), and NIH Grants CA 90571 and CA107300 (to M.A.T.). The GC/MS Facility at Harbor-University of California Los Angeles (UCLA) was supported by Public Health Service Grant P01-CA42710 to the UCLA Clinical Nutrition Research Unit and Grant M01-RR00425 to the Harbor-UCLA General Clinical Research Center. M.A.T. was also supported by the Margaret E. Early Medical Research Trust and CMISE with a NASA URETI award NCC 2-1364. M.A.T. is a scholar of the Leukemia and Lymphoma Society.

REFERENCES

- Accili D: Lilly Lecture 2003: The struggle for mastery in insulin action: from triumvirate to republic. *Diabetes* 53:1633–1642, 2004
- Michael MD, Kulkarni RN, Postic C, Previs SF, Shulman GI, Magnuson MA, Kahn CR: Loss of insulin signaling in hepatocytes leads to severe insulin resistance and progressive hepatic dysfunction. *Mol Cell* 6:87–97, 2000
- Fisher SJ, Kahn CR: Insulin signaling is required for insulin's direct and indirect action on hepatic glucose production. *J Clin Invest* 111:463–468, 2003
- Buettner C, Patel R, Muse ED, Bhanot S, Monia BP, McKay R, Obici S, Rossetti L: Severe impairment in liver insulin signaling fails to alter hepatic insulin action in conscious mice. *J Clin Invest* 115:1306–1313, 2005
- Zhou QL, Park JG, Jiang ZY, Holik JJ, Mitra P, Semiz S, Guilherme A, Powelka AM, Tang X, Virbasius J, Czech MP: Analysis of insulin signalling by RNAi-based gene silencing. *Biochem Soc Trans* 32:817–821, 2004
- Tang X, Powelka AM, Soriano NA, Czech MP, Guilherme A: PTEN, but not SHIP2, suppresses insulin signaling through the phosphatidylinositol 3-kinase/Akt pathway in 3T3-L1 adipocytes. *J Biol Chem* 280:22523–22529, 2005
- Wada T, Sasaoka T, Funaki M, Hori H, Murakami S, Ishiki M, Haruta T, Asano T, Ogawa W, Ishihara H, Kobayashi M: Overexpression of SH2-containing inositol phosphatase 2 results in negative regulation of insulin-induced metabolic actions in 3T3-L1 adipocytes via its 5'-phosphatase catalytic activity. *Mol Cell Biol* 21:1633–1646, 2001
- Sleeman MW, Wortley KE, Lai KM, Gowen LC, Kintner J, Kline WO, Garcia K, Stitt TN, Yancopoulos GD, Wiegand SJ, Glass DJ: Absence of the lipid phosphatase SHIP2 confers resistance to dietary obesity. *Nat Med* 11:199–205, 2005
- Butler M, McKay RA, Popoff IJ, Gaarde WA, Witchell D, Murray SF, Dean NM, Bhanot S, Monia BP: Specific inhibition of *PTEN* expression reverses hyperglycemia in diabetic mice. *Diabetes* 51:1028–1034, 2002
- Wijesekara N, Konrad D, Eweida M, Jefferies C, Liadis N, Giacca A, Crackower M, Suzuki A, Mak TW, Kahn CR, Klip A, Woo M: Muscle-specific *Pten* deletion protects against insulin resistance and diabetes. *Mol Cell Biol* 25:1135–1145, 2005
- Kushner JA, Simpson L, Wartschow LM, Guo S, Rankin MM, Parsons R, White MF: Phosphatase and tensin homolog regulation of insulin growth and glucose homeostasis. *J Biol Chem* 280:39388–39393, 2005
- Kurlawalla-Martinez C, Stiles B, Wang Y, Devaskar SU, Kahn BB, Wu H: Insulin hypersensitivity and resistance to streptozotocin-induced diabetes in mice lacking *PTEN* in adipose tissue. *Mol Cell Biol* 25:2498–2510, 2005
- Stiles B, Wang Y, Stahl A, Bassilian S, Lee WP, Kim YJ, Sherwin R, Devaskar S, Lesche R, Magnuson MA, Wu H: Liver-specific deletion of negative regulator *Pten* results in fatty liver and insulin hypersensitivity. *Proc Natl Acad Sci U S A* 101:2082–2087, 2004
- Horie Y, Suzuki A, Kataoka E, Sasaki T, Hamada K, Sasaki J, Mizuno K, Hasegawa G, Kishimoto H, Iizuka M, Naito M, Enomoto K, Watanabe S, Mak TW, Nakano: Hepatocyte-specific *Pten* deficiency results in steatohepatitis and hepatocellular carcinomas. *J Clin Invest* 113:1774–1783, 2004
- Xu J, Xiao G, Trujillo C, Chang V, Blanco L, Joseph SB, Bassilian S, Saad MF, Tontonoz P, Lee WN, Kurland IJ: Peroxisome proliferator-activated receptor alpha (PPARalpha) influences substrate utilization for hepatic glucose production. *J Biol Chem* 277:50237–50244, 2002
- Xu J, Lee WN, Xiao G, Trujillo C, Chang V, Blanco L, Hernandez F, Chung B, Makabi S, Ahmed S, Bassilian S, Saad M, Kurland IJ: Determination of a glucose-dependent futile recycling rate constant from an intraperitoneal glucose tolerance test. *Anal Biochem* 315:238–246, 2003
- Xu J, Chang V, Joseph SB, Trujillo C, Bassilian S, Saad MF, Lee WN, Kurland IJ: Peroxisomal proliferator-activated receptor alpha deficiency diminishes insulin-responsiveness of gluconeogenic/glycolytic/pentose gene expression and substrate cycle flux. *Endocrinology* 145:1087–1095, 2004
- Podsypanina K, Ellenson LH, Nemes A, Gu J, Tamura M, Yamada KM, Cordon-Cardo C, Catorretti G, Fisher PE, Parsons R: Mutation of *Pten/Mmac1* in mice causes neoplasia in multiple organ systems. *Proc Natl Acad Sci U S A* 96:1563–1568, 1999
- Sun H, Lesche R, Li DM, Liliental J, Zhang H, Gao J, Gavrilova N, Mueller B, Liu X, Wu H: *PTEN* modulates cell cycle progression and cell survival by regulating phosphatidylinositol 3,4,5-trisphosphate and Akt/protein kinase B signaling pathway. *Proc Natl Acad Sci U S A* 96:6199–204, 1999
- Sleeman MW, Garcia K, Liu R, Murray JD, Malinova L, Moncrieffe M, Yancopoulos GD, Wiegand SJ: Ciliary neurotrophic factor improves diabetic parameters and hepatic steatosis and increases basal metabolic rate in db/db mice. *Proc Natl Acad Sci U S A* 100:14297–14302, 2003
- Wolfe RR, Chinkes DL: *Isotope Tracers in Metabolic Research*. 2nd ed. New York, Wiley, 2005
- Kurland IJ, Lee WN, Saad MF, Xu J: The hepatic recycling glucose tolerance test (HR-GTT)[article online], 2002. Available from <http://www.research.ucla.edu/tech/ucla02-318.htm>. Accessed 26 October 2006
- Vranic M: Banting Lecture: Glucose turnover: a key to understanding the pathogenesis of diabetes (indirect effects of insulin). *Diabetes* 41:1188–1206, 1992
- Roth U, Curth K, Unterman TG, Kietzmann T: The transcription factors HIF-1 and HNF-4 and the coactivator p300 are involved in insulin-regulated glucokinase gene expression via the phosphatidylinositol 3-kinase/protein kinase B pathway. *J Biol Chem* 279:2623–2631, 2004
- O'Brien RM, Streeper RS, Ayala JE, Stadelmaier BT, Hornbuckle LA: Insulin-regulated gene expression. *Biochem Soc Trans* 29:552–558, 2001
- Vander Kooi BT, Streeper RS, Svitek CA, Oeser JK, Powell DR, O'Brien RM: The three insulin response sequences in the glucose-6-phosphatase catalytic subunit gene promoter are functionally distinct. *J Biol Chem* 278:11782–11793, 2003
- Burgess SC, Malloy CR, Sherry DA, Linder J, Magnuson MA: Metabolic control of PEPCK on gluconeogenesis (Abstract). *Diabetes* 55 (Suppl. 1):A351, 2006
- Burgess SC, Hausler N, Merritt M, Jeffrey FM, Storey C, Milde A, Koshy S, Lindner J, Magnuson MA, Malloy CR, Sherry AD: Impaired tricarboxylic acid cycle activity in mouse livers lacking cytosolic phosphoenolpyruvate carboxykinase. *J Biol Chem* 279:48941–48949, 2004
- Hakimi P, Johnson MT, Yang J, Lepage DF, Conlon RA, Kalhan SC, Reshef L, Tilghman SM, Hanson RW: Phosphoenolpyruvate carboxykinase and the critical role of cataplerosis in the control of hepatic metabolism. *Nutr Metab (Lond)* 2:33, 2005
- Landau BR: Glycerol production and utilization measured using stable isotopes. *Proc Nutr Soc* 58:973–978, 1999
- Jensen MD, Chandramouli V, Schumann WC, Ekberg K, Previs SF, Gupta S, Landau BR: Sources of blood glycerol during fasting. *Am J Physiol Endocrinol Metab* 281:E998–E1004, 2001